THE JOURNAL OF PHYSICAL CHEMISTRY B

Article

pubs.acs.org/JPCB

Molecular Dynamics Simulations of Human Serum Albumin and Role of Disulfide Bonds

Maria Monica Castellanos and Coray M. Colina*

Department of Materials Science and Engineering, The Pennsylvania State University, University Park, Pennsylvania 16802, United States

Supporting Information

ABSTRACT: Atomistic molecular dynamics simulations of human serum albumin in the presence and absence of disulfide bonds are presented. Simulations of 70 ns duration provide information on the relevance of disulfide bonds in the dynamics and structural conformation of HSA. Significant conformational changes are observed in the absence of disulfide bonds after 35 ns that could impact the functionality and stability of the protein. Changes in the secondary structure, hydrogen bonds, *B* factors, and cross-correlations reveal which disulfide bonds are important for keeping the secondary and tertiary structure and dynamics of the protein (e.g., Cys168−Cys177, Cys278−Cys289) and which have little effect on the local structure and dynamics (e.g., Cys200−Cys246, Cys461−Cys477). Removing all disulfide bonds in the protein appears to be a practical prescreening tool for identifying disulfide bonds relevant to structure and dynamics. In the absence of disulfide bonds, certain hydrogen bonds and correlated motions vanish, affecting the structure of neighboring residues. The structure of the primary binding sites of HSA is partially affected when disulfide bonds are removed. For the native structure, simulations clearly reveal the conformational changes that allow the only free cysteine to be exposed on the protein surface to form intermolecular disulfide bonds; this information could not be resolved from the static crystal structure alone. The absence of specific disulfide bonds could lead to partially unfolded structures; such structures are known to be prone to protein aggregation. Removing disulfide bonds could have similar consequences in other proteins of interest, such as immunoglobulin G.

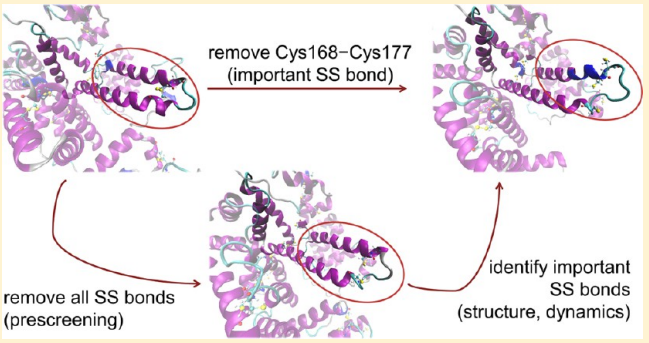

1. INTRODUCTION

Disulfide bonds (SS bonds), also known as disulfide bridges, are covalent bonds that have been observed to play an important role in protein stability and aggregation.[1] SS bonds are formed by a thiol/disulfide exchange reaction, and three important factors are required in the reactive groups to form this bond: accessibility, proximity, and reactivity (electrostatic environment).[2−5] Creighton[4] presented three unique stereochemical requirements that should be satisfied for cysteine residues to be involved in SS bonds: (1) a distance of 2.05 ± 0.03 Å between sulfur atoms, (2) an angle between the sulfur atoms forming the SS bond and each β-carbon atom close to 103°, and (3) an orientation of the two β-carbon atoms corresponding to a rotation of ±90° about the SS bond. Two sulfur atoms have interactions on the order of 300−430 kJ/mol,[5] and therefore, the absence of this interaction is expected to produce significant structural changes in the conformation of the protein. Conformational changes in serum albumin related to the loosening of the structure were observed in conditions where attractive protein interactions dominated,[6] indicating that a significant change in conformation could lead to the formation of protein aggregates.

During the in vivo folding process, the formation and breakage of SS bonds is catalyzed by a protein disulfide isomerase.[7] Experimentally, SS bonds can be removed with reducing agents such as β-mercaptoethanol and dithiothreitol, and their formation is prevented by inhibitors such as iodoacetamide or iodoacetic acid.[8−10] SS bonds play different roles in maintaining structure, stability, and functionality. The effect of SS bonds on the structure and dynamics of different proteins has been a subject of interest experimentally[11−14] and computationally.[15−20] Some of the consequences of removing disulfide bonds include a decrease in the stability of the unfolded state,[11] changes in the formation of correct SS bond pairs,[12] and a localized destabilization and decrease in activity.[13]

In the area of protein design and engineering, experimental techniques have been developed to study the stability of proteins, disruption or blockage of sulfhydryl groups in cysteine residues, and addition of SS bonds.[17,19−21] Limited success has been achieved by the addition of SS bonds, and a decrease of stability has occurred.[4,22,23] Studies performed on fragments of

Received: March 26, 2013
Revised: September 4, 2013

   dx.doi.org/10.1021/jp402994r | J. Phys. Chem. B XXXX, XXX, XXX−XXX

antibodies have shown that the absence of SS bonds influences the stability and aggregation propensity of antibody domains significantly, whereas the folding of domains is not substantially affected.[24]

For many proteins in the native state, most sulfhydryl groups are forming SS bonds, but free cysteine residues have been detected in proteins such as immunoglobulin G (IgG) under denaturing conditions.[25] As a first step toward understanding aggregation, human serum albumin (HSA) is used here as a model protein to show potential changes in structure and dynamics that could occur as a result of free cysteine residues not forming SS bonds. The HSA atomistic simulations presented in this work are computationally an order of magnitude faster than what a molecular simulation of a high-molecular-weight protein such as IgG1 would demand. Although IgG and HSA are very different molecules, both proteins have significant numbers of SS bond pairs connecting regions in the same domain, and changes similar to those observed in this work might occur in other proteins with significant numbers of SS bonds. Protein aggregates from structures forming intermolecular SS bonds have been observed,[26−31] and understanding SS bonds at the atomistic level and their effects on native conformations is a necessary step to further understanding protein aggregation at longer time and length scales.

Because experimental techniques used for the modification of SS bonds require extreme care, particularly to avoid steric and polarity clashes,[22] atomistic molecular simulations are an alternative approach to easily modify the protein and determine changes in structure and dynamics. Molecular dynamics (MD) simulations have been used to study the effects of SS bonds on the structural properties of a variety of molecules such as hepcidins,[19] lipid-transfer proteins,[20] tendamistat,[17] and barnase.[21] In general, SS bonds are important to maintain tertiary structure and protein dynamics, particularly when folding pathways are disrupted in the absence of SS bonds. Atomistic simulations offer the further advantage of generating a database of conformational structures of a single protein that can be used in the development of accurate coarse-grained mesoscale models[32] (i.e., bottom-up approach) to study other phenomena of interest such as protein aggregation.[33,34]

The purpose of this study was threefold: (1) to elucidate the effect of removing SS bonds of HSA on the local and overall structure, flexibility, and correlated motions; (2) to determine how key local residues previously identified to play a role in functionality and binding affinity are affected by the absence of SS bonds; and (3) to study the native structure and generate a databank of structures for the development of mesoscale models to understand protein aggregation.

This study reveals conformational changes in the HSA native structure when SS bonds are removed. For the simulation time studied (70 ns), not all SS bonds were essential to maintain structure, and some regions with cysteine residues still conserved a nativelike structure when SS bonds were not present. The free Cys34 in the native form of HSA was observed to be accessible from the surface by conformational changes of the bulky Tyr84 residue. This study will be of great relevance for understanding the effects of removing disulfide interactions in proteins, which is expected to have a significant effect on macroscopic behaviors of interest, such as protein aggregation.

2. SIMULATION SETUP

Atomistic MD simulations were performed with the Amber 12 simulation package implemented in CUDA-enabled NVIDIA graphics processing units (GPUs).[35,36] The crystallographic structure (PDB entry 1AO6)[37] of two nonfatted HSA with seven crystallographic waters molecules at a resolution of 2.5 Å was used. Structures with and without SS bonds were generated by creating the corresponding topology and coordinate files using TLEAP with the Amber 99SB force field. In particular, the following five cases were studied: all SS bonds maintained (native structure), all SS bonds removed, removal of SS bond Cys168−Cys177 and its corresponding pair (Cys124−Cys169) simultaneously, and removal of Cys124−Cys169 and Cys168−Cys177 separately. Fifteen sodium counterions were added to neutralize charges in the protein. The protein was solvated with explicit TIP3P water, with a buffering distance of 20 Å in an octahedral box. Each system contained a total of 148636 atoms.

Energy minimizations were implemented in the Sander module in two steps: (1) The protein was first restrained while water minimization was performed, and then (2) minimization of the whole system was performed. Minimization of water was implemented in 10000 steps, using steepest descent before applying the conjugate gradient method. The cutoff for nonbonded interactions was set to 12 Å. Minimization of the whole system was completed similarly in 20000 steps.

MD simulations were performed for 70 ns with the PMEMD Amber implementation tool. Before *NPT* simulations were run, the temperature of the system was raised slowly from 0 to 300 K for 80 ps, using the Berendsen coupling algorithm.[38] This procedure was followed by a 50 ps *NVT* simulation. For the *NPT* simulations, the temperature was maintained at 300 K using the Langevin dynamics algorithm[39−41] with a collision frequency of 2.0. Periodic boundary conditions were applied with a constant pressure of 1 atm and a pressure relaxation time of 2 ps. For all MD simulations, bond-length constraints on the hydrogen atoms were applied using the SHAKE algorithm.[42] The time step was 1 fs, and information for analysis was printed every 10 ps. The nonbonded list was updated every 10 steps using a cutoff distance of 9 Å. Long-range interactions were considered using the particle mesh Ewald algorithm.[43−45] Analysis of the trajectories was conducted using the PTRAJ module of Amber.

3. RESULTS AND DISCUSSION

HSA is the most abundant protein in the bloodstream at concentrations of 50 mg/mL. It is also present in lymph, chyle, cellular tissues, and aqueous and vitreous humor, as well as tissue extracts and body fluids such as synovial and cerebrospinal fluid.[46,47] Serum albumin helps to maintain the osmotic pressure of the body and is an important carrier of fatty acids, metabolites, drugs and other important ligands.[47−50] Drug interactions with HSA are relevant for the pharmacokinetic properties of a variety of drugs.[51−58] HSA is one of the most relevant human proteins and understanding its structure, dynamics, binding affinity, functionality and aggregation propensity has an enormous impact in drug delivery applications.[56,57,59]

HSA has a predominant α-helix heart-shaped structure with 585 residues.[48,60] It is usually divided into three homologous domains, each with two subdomains: IA (residues 1−107), IB (residues 108−195), IIA (residues 196−297), IIB (residues 298−383), IIIA (residues 384−497), and IIIB (residues 498−

dx.doi.org/10.1021/jp402994r | J. Phys. Chem. B XXXX, XXX, XXX−XXX

585).[37] Subdomains IIA and IIIA are known as the primary binding sites, although fatty acids also bind to many other regions of the protein.[61] SS bonds in HSA are uniformly distributed in all of the protein domains, with two to four residues in each subdomain. There are 17 SS bonds, and 16 of them form the so-called double SS bonds as they are next to each other in the amino acid sequence. There is a free cysteine (Cys34) that participates in intermolecular SS bonds forming dimers.[62] Nevertheless, in the crystal structures (1AO6[37] and 1N5U[63]), this cysteine is surrounded by other residues and hardly accessible from the surface, preventing coupling with other cysteine groups. The structure and distribution of SS bonds in HSA are shown in Figure 1. SS bonds do not connect different domains of HSA, but adjoin helical segments with a coil structure between them.

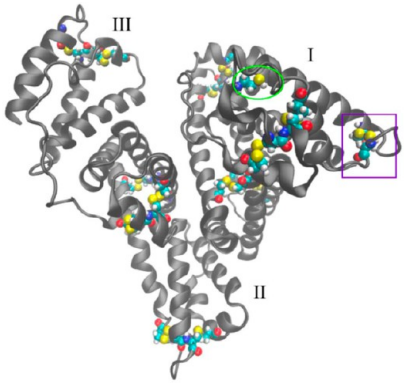

Figure 1. Cartoon representation of human serum albumin (PDB entry 1AO6).[37] Disulfide bonds are represented as van der Waals (vdW) spheres. Sulfur atoms are in yellow. Eight SS bonds are located in the primary binding sites (four in each subdomain). There is a free cysteine group (Cys34, green circle) and a SS bond that does not form a double SS bond (Cys53−Cys62, purple square). The cartoon was created using Visual Molecular Dynamics (VMD).[64]

3.1. Effect of Disulfide Bonds on Protein Conformation. HSA has been largely recognized as a flexible molecule having the ability to explore different conformations.[65,66] Root-mean-square deviations (RMSDs) provide insights into the conformational changes of the structure by comparing changes in the positions of the atoms with a reference structure. RMSDs were calculated with respect to the initial crystal structure for the structures with and without SS bonds (Figure 2). During the first 15 ns both structures changed significantly with respect to the crystal structure (~3 Å). After ~15 ns, no significant changes in the RMSD are observed for the native structure. Starting at about 15 ns and for about 20 ns, the structure without SS bonds reaches a plateau, having RMSD values only slightly higher than 3 Å. The structure without SS bonds shows a conformational change from the stable native conformation after ~35 ns. This is possibly due to metastable states or lower energy barriers in the protein landscape when SS bonds are removed. The RMSD values for the simulated structure with SS bonds are about 1 Å lower than in the absence of them.

Previous MD studies in HSA and its ligand affinity reported RMSD values at Cα for time frames from 1 up to 10 ns.[67−72] Artali et al.[72] ran a 5 ns MD simulation, starting from the same crystal structure used in this study (PDB entry 1AO6),[37] using the GROMOS96 force field reporting only the last 2 ns, with RMSD values ranging from 3.3 to 5.6 Å. Li et al.[67] used

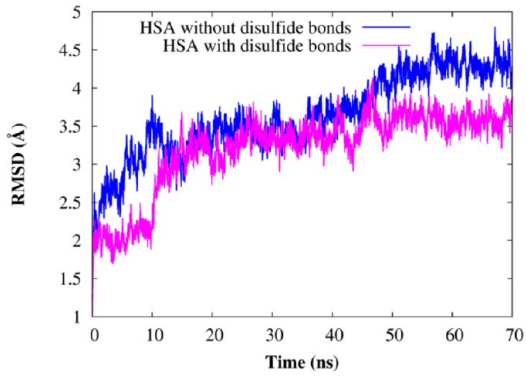

Figure 2. Evolution over 70 ns of the RMSD at Cα for structures of HSA with and without SS bonds, referenced to the crystal structure (1AO6).[37] Both MD-simulated structures reach a plateau in the RMSD after about 15 ns. The structure with SS bonds keeps its conformation and stability during the remainder of the simulation, whereas the structure without SS bonds experiences changes in conformation after 35 ns.

different starting PDB entries (1HZ9[59] and 1E7A[73]) of the noncomplexed HSA and the GROMOS96 force field, obtaining stable values in the RMSD after about 2 ns for a 10 ns run, with average RMSD values of 4.5 Å. Similarly, Fujiwara et al.[68] ran a MD simulation for 10 ns, with the AMBER94 force field and the same starting structure of the present work (1AO6),[37] with RMSD values ranging from 3 to 4.5 Å. All these results are consistent with the simulation of the unmodified structure of this study. Sudhamalla et al.[69] found RMSD values from 4 up to 9 Å in a 6 ns simulation starting from the same initial conformation (PDB entry 1AO6),[37] where the main difference appears to be related with the force field selected (GROMOS 96 43a1).[70] Deeb et. al[71] reported RMSD values from 2 to 3 Å during a 5 ns MD simulation; these values are closer to the first 10 ns results of the simulated structure with SS bonds and longer simulations might have revealed similar results as the ones obtained here for 70 ns.

3.2. Conformational Stability in the Absence of Disulfide Bonds. Secondary structural changes can be assigned in a quantitative manner based on the definitions of DSSP by Kabsch and Sander or STRIDE by Frishman and Argos.[74,75] Both algorithms were used in this work, along with visual inspection of snapshots to merge these methods. In the absence of SS bonds, the secondary structure of the protein is generally maintained, except in specific regions where some α-helices unfold. In particular, unfolding of α-helices was observed in domains IB and IIIB in the regions between Cys168 and Cys177 and between Cys558 and Cys567, respectively. The secondary structure is partially affected in the main binding sites, such as in the α-helices formed by residues Glu227-Gln268 in domain IIA as discussed below. Changes in local structure were observed when the sulfhydryl in cysteine moved far apart from its corresponding cysteine pair.

The analysis of distances between sulfur atoms (Sγ) in pairs of cysteines was an important tool to identify the effect of removing each SS bond on the structural stability, correlated motion and flexibility of local residues. In the absence of SS bonds, most pairs of Sγ atoms have regions with a preferred distance of about 4.1 Å (standard deviation of 0.5 Å), suggesting that they sample conformations with some probability of forming a bond again. In the present atomistic simulations and with the selected force field, the formation of a

dx.doi.org/10.1021/jp402994r | J. Phys. Chem. B XXXX, XXX, XXX−XXX

covalent bond cannot be studied once it has been broken. However, it is possible to identify pairs of sulfhydryl groups −SH that once their bonds have been broken, their separation distance increases significantly and thus have a lower probability of forming a bond again. As an example, Figure 3

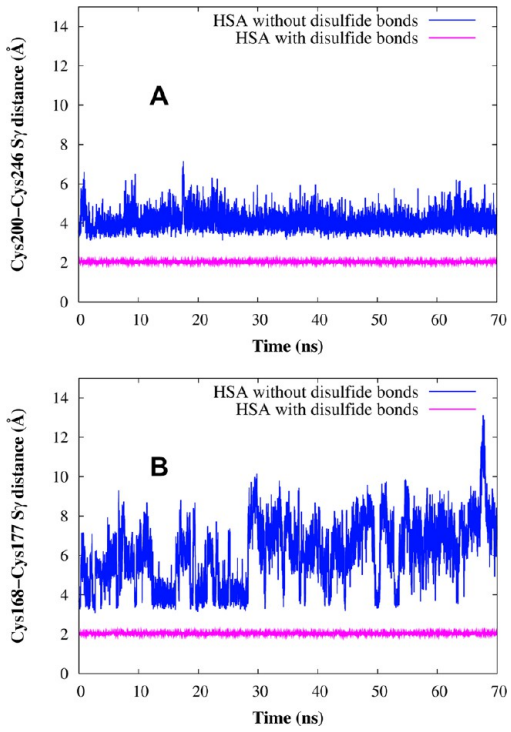

Figure 3. Separation of cysteine Sγ atoms in the absence of SS bonds. Two examples are presented (in blue) and compared to the distance of the simulated structure with SS bonds (in pink): (A) Cys200−Cys246 and (B) Cys168−Cys177. Not all SS bonds provide structure to HSA as in Cys200−Cys246, which conserved a stable separation throughout the simulation. Even when the physical bond is removed, other interactions keep them stable within a distance at which they have chances to form a bond again. However, once the bond between Cys168 and Cys177 has been removed, these cysteine residues separate and sample different conformations, while decreasing the probability of forming a bond again.

represents a comparison between a SS bond that is stable (Cys200−Cys246) compared to Cys168−Cys177 that samples separations far from the native equilibrium distance (2.03 Å). Additional figures of the distances sampled by each SS bond (from their Sγ atom) can be found in the Supporting Information (Figures SI.1−SI.3). Importantly, we found that most pairs of cysteine residues are stable (i.e., stay at a "constant" separation) in the absence of the SS bonds, as in Cys75−Cys91, Cys200−Cys246, Cys360−Cys369, and Cys461−Cys477. Because they sample distances around 4.1 Å, it is likely that they form a SS bond again. In contrast, the distances between the pairs of residues Cys168−Cys177, Cys437−Cys448 and Cys558−Cys567 fluctuate considerably in the absence of SS bonds, and significant changes in the secondary structure of local residues were observed. Less pronounced fluctuations and partial variations in structure and dynamics are observed for Cys245−Cys253 and Cys265−Cys279, with separations of ∼5 Å and mostly below 10 Å (see Figures SI.1−SI.3, Supporting Information). Cys278−Cys289 and Cys392−Cys438 reach stable conformations at distances above 5 Å, where the interaction between sulfhydryl groups is expected to be weaker.

For many protein engineering applications, only a single or a few SS bonds are removed and it becomes of interest to elucidate how much this disruption will affect the structural stability and dynamics of the protein. Based on the results from the simulation when all SS bonds are removed, it was hypothesized that the SS bond formed by Cys168−Cys177 plays an important role in the structure and dynamics of HSA. The effect of removing Cys168−Cys177 and Cys124−169 (both pairs form a double SS bond) simultaneously and separately were also studied.

Figure 4 shows the RMSD for the whole protein calculated with respect to the crystal structure (1AO6) for the 5 cases

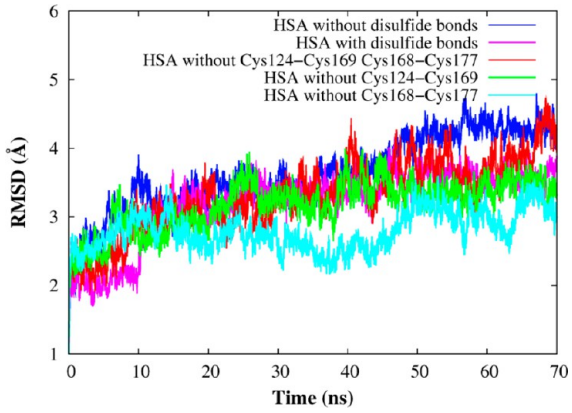

Figure 4. RMSDs for the five cases studied in this work. Results in the absence of SS bond(s) Cys124−Cys169, Cys168−Cys177, or both are in close agreement with the native structure (all SS bonds present).

studied in this work. No significant changes are observed when only Cys124−Cys177 is removed compared to the structure in which all SS bonds are present. Some differences occurred for the case when only Cys168−Cys177 is removed, but after 50 ns it reaches similar values as the other cases studied. In general, removing only Cys124−Cys177, Cys168−Cys177 or both produce an overall conformation similar to the native structure with all SS bonds present during the 70 ns trajectory.

Figure 5 depicts the distances between the Sγ atoms in Cys168−Cys177. The conformation sampled in the absence of the SS bond Cys168−Cys177 is mostly consistent with the first 30 ns of MD with all SS bonds removed. When both Cys124−169 and Cys168−Cys177 are absent, the conformation sampled by the SS bond Cys168−Cys177 agrees with results after 30 ns when all SS bonds are removed. These results show that a Sγ distance of ∼4.1 Å and beyond (up to 15 Å) could be explored when Cys168−Cys177 is removed and significant changes in the local structure and dynamics will occur.

Similar comparisons were established for the SS bond between Cys124 and Cys169 and results are presented in Figure 6. Results are very consistent when either the SS bond Cys124−Cys169 or all SS bonds are removed. However when Cys124−Cys169 and Cys168−Cys177 are absent, the Sγ distance in Cys124−Cys169 increases dramatically reaching values up to 15 Å, suggesting that some double SS bonds (consecutive cysteine residues in the aminoacid sequence) are important for the local secondary structure.

The present study elucidates that the most susceptible SS bonds can be identified from a simulation with all SS bonds

dx.doi.org/10.1021/jp402994r | J. Phys. Chem. B XXXX, XXX, XXX−XXX

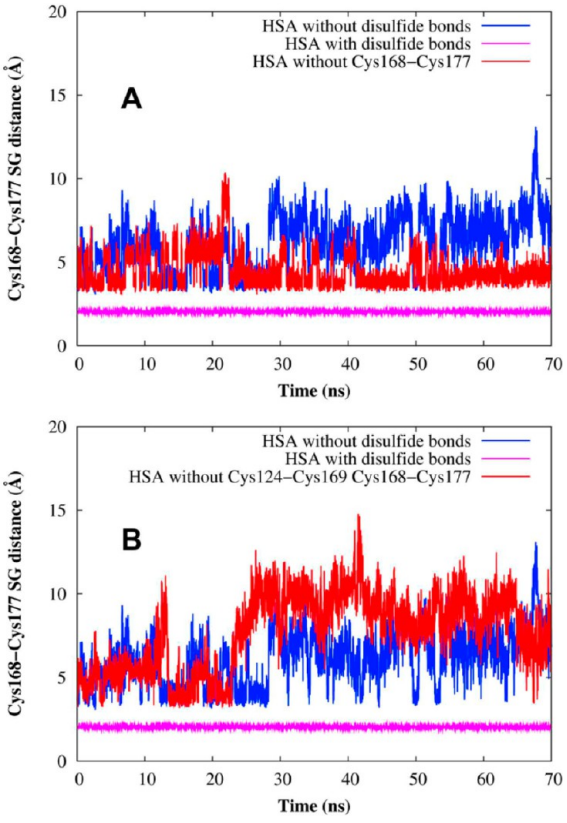

Figure 5. Separation of cysteine Sγ atoms in Cys168−Cys177 after removal of (A) the SS bond Cys168−Cys177 and (B) the double SS bond at Cys124−Cys169 and Cys168−Cys177. For comparison purposes, results with all SS bonds removed (blue) and all SS bonds present (pink) are included. Similar distances were sampled in all simulations where the SS bond Cys168−Cys177 is absent.

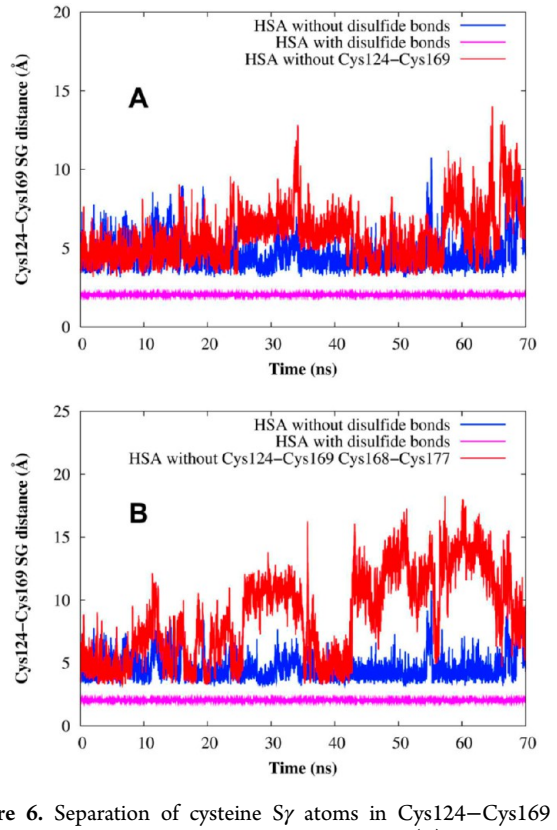

Figure 6. Separation of cysteine Sγ atoms in Cys124−Cys169 (A) when the SS bond Cys124−Cys169 is absent and (B) after removal of the double SS bond at Cys124−Cys169 and Cys168−Cys177. For comparison purposes, results with all SS bonds removed (blue) and all SS bonds present (pink) are included. In the absence of the double SS bond, a pronounced increase in the distance occurs, suggesting a significant structural change in the local residues.

broken. This is an important finding because a molecular simulation with all SS bonds removed can be used as a prescreening tool to identify which SS bonds are more prone to affect the protein structure and dynamics. After these SS bonds have been identified, a more comprehensive study in the absence of specific SS bonds can be performed, avoiding a systematic and expensive study (both computationally and experimentally) of breaking each SS bond.

3.3. Protein Dynamics. Besides affecting the size and shape of HSA, the absence of SS bonds changed the local dynamics. In Figure 7, *B* factors (temperature factors) are plotted for each residue with and without SS bonds and compared to *B* factors obtained from the X-ray 1AO6[37] crystal structure. For clarity purposes and as fluctuations are stronger for longer time frames, these *B* factors correspond to a trajectory of 5 ns in the time frame of 65 to 70 ns, which correspond to equilibrated trajectories according to the plateau in the RMSD. Similar trends are observed among the MD simulations and the experimental crystal structure. In particular, the binding sites (subdomains IIA and IIIA) have low *B* factors, as observed in other studies,[68,69,72] even when the four SS bonds in each binding site are not present (i.e., the absence of SS bonds does not severely affect the dynamics of the binding sites). Additionally, sharp peaks are found in subdomain IB as the absence of the Cys168−Cys177 SS bond creates a very flexible region, where separations between the sulfur atoms could reach up to 10 Å. The absence of this SS bond promotes a change in secondary structure and dynamics where some α-helices unfold into coils, and thus appears to be responsible for providing structural stability to local regions.

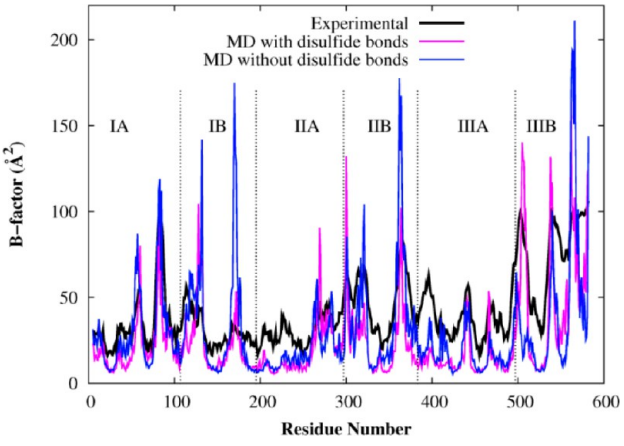

Figure 7. *B* factors at Cα for 5-ns MD trajectories of HSA with and without SS bonds, compared to the experimental crystal structure. The main binding sites (residues 196−297 for site I and 384−497 for site II) form rigid regions compared to other residues in the protein. A strong peak between residues 150 and 200 arises in the structure without SS bonds, whereas the same peak is weaker for the structure with SS bonds. The absence of the SS bonds between Cys168 and Cys177 promotes unfolding of α-helices in domain IB and changes in secondary structure.

dx.doi.org/10.1021/jp402994r | J. Phys. Chem. B XXXX, XXX, XXX−XXX

A cross-correlation analysis[76] provides information on the similarity or correlated spatial motion between the C_α of a pair of residues and is calculated as:

$$C_{ij} = \frac{\langle \Delta r_i \cdot \Delta r_j \rangle}{\sqrt{\langle \Delta r_i \rangle^2 \langle \Delta r_j \rangle^2}} \quad (1)$$

where Δr_i corresponds to the displacement of atom i compared to a reference position. The values of the cross-correlation vary from −1 to 1 for motions completely anticorrelated and correlated respectively. By visual pattern recognition, a dynamic cross-correlation map (DCCM) provides information on the similarity or correlated spatial motion between a pair of residues. A DCCM was generated from trajectories with and without SS bonds and is presented in Figure 8, where a red color is indicative of a strong cooperative motion between residues, and a dark blue indicates a negative correlation. Inspection of both graphs clearly reveals the regions in which correlated motions are affected by the absence of SS bonds. For completeness, the most significant changes when comparing the DCCM with and without SS bonds are listed in the Supporting Information. As an example, a covariance analysis indicates that the first SS bond in the sequence and the only nonpaired SS bond (Cys53−Cys62) has correlated motions with the region formed by Ser5 and His9. The region near Cys514−Cys559 and Cys558−Cys567 has strong correlations with residues in their vicinity such as Asn503-Glu505 and Glu542−Cys559, which weaken in the absence of SS bonds. The removal of SS bonds affected a number of correlated motions such as those in residues Glu119−Cys124 and Cys169−Ala175, Glu131−Thr133 and Ala504−Phe507. However, the absence of SS bonds also induced stronger correlate motions, as in the regions encompassed by residues Lys199−Gln204, Leu408−Thr412, Thr506−His510. When SS bonds are removed some hydrogen bonds strengthen, preventing significant unfolding and abrupt changes in conformational structure and dynamics, suggesting that other interactions become important when SS bonds are absent. In general, removing SS bonds either decreased or removed correlated motions in the neighborhood where SS bonds are present, with a few exceptions (Cys200−Cys246 and Cys245−Cys253 have no correlated motions in either case; correlated motions in Cys316−Cys361 and Cys360−Cys369 are not significantly affected).

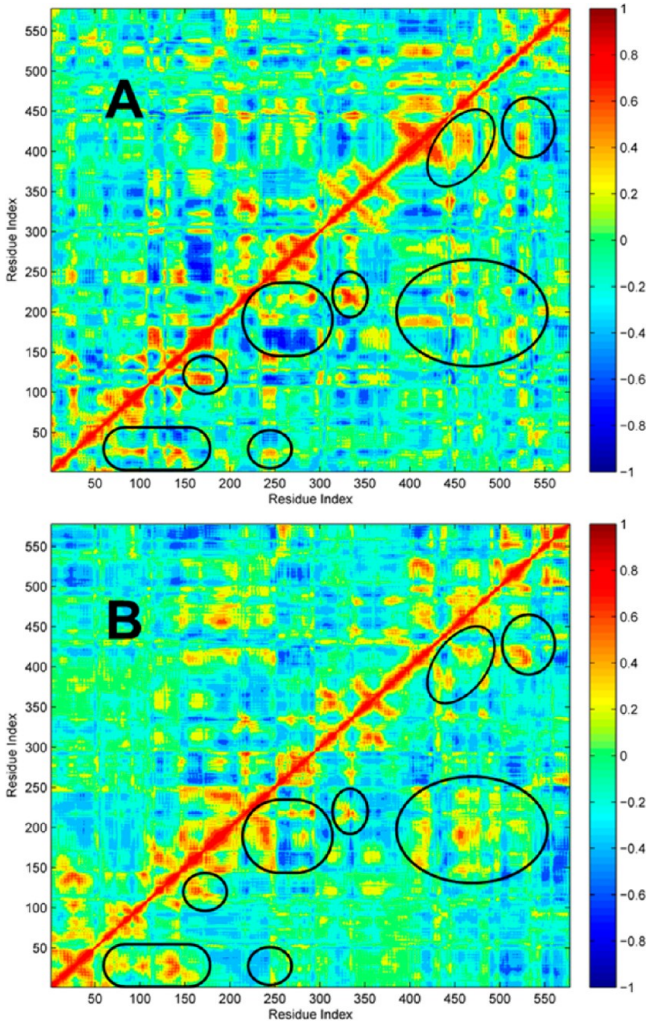

Figure 8. Dynamic cross-correlation maps of HSA in the (A) presence and (B) absence of SS bonds. Correlated motions are affected differently when SS bonds are removed. Some correlations and specific hydrogen bonds vanish or become weak when SS bonds are removed, as in the local region enclosed by the SS bond between Cys53 and Cys62. Nevertheless, stronger correlated motions were also observed when SS bonds were removed, such as in Leu408-Thr412. Intramolecular interactions contribute to the dynamical response and structure of HSA, allowing only partial changes when SS bonds are removed.

Regions where other noncovalent interactions (hydrogen bonds, salt bridges, etc.) are responsible for preventing severe changes in secondary structure and correlated motion were identified. In particular, correlations between the DCCM and hydrogen-bond interactions were established. The correlated motion of residue Gln221−Ala226 with residues Ile271−Lys274 and Val293−Met298 is not affected by the rupture of local SS bonds (there are four of them in this section of subdomain IIA), but hydrogen bonds are responsible for keeping a correlated motion and the structure of these regions. Hydrogen bonds between the pairs of residues Val216−Ser220, Ala226−Tyr332, and Ser273−Asp296 still keep occupancies from 97%, 99% and 99% in the absence of SS bonds respectively (see Supporting Information). Similarly, hydrogen bonds are maintained when SS bonds are removed, such as in Glu48−Thr52, Gln32−Arg144 and Pro303−Arg337. The region formed by Leu529−Pro537 in domain III has correlated motions with residues in the same domain when SS bonds are absent, which are weaker when SS bonds are present. New hydrogen bonds are observed between the pairs of residues Gln29−Phe149, Tyr150−Asp249, Ser312−Tyr370, and Thr420−Glu531 that do not have significant occupancies (less than 60%) in the native state.

3.4. Surface Accessibility of Cys34 in HSA. Cys34 is the only cysteine with a free sulfhydryl group in HSA, and it has been identified as a metal-binding site.[48] About 30% of this sulfhydryl is oxidized by cysteine and glutathione in the bloodstream and it can participate in an intermolecular SS bonds forming dimers.[62] Sugio et al.[37] did not observe a surface accessible Cys34 in their X-ray crystal structure, as the Sγ atom was hindered by side groups of Pro35, His39, Val77 and Tyr84. They hypothesized that the sulfhydryl group Cys34 would be able to link with other sulfhydryl groups when the phenolic side of Tyr84 "flips over" or there is a change in backbone conformation, exposing Cys34 to the surface. MD simulations

dx.doi.org/10.1021/jp402994r | J. Phys. Chem. B XXXX, XXX, XXX−XXX

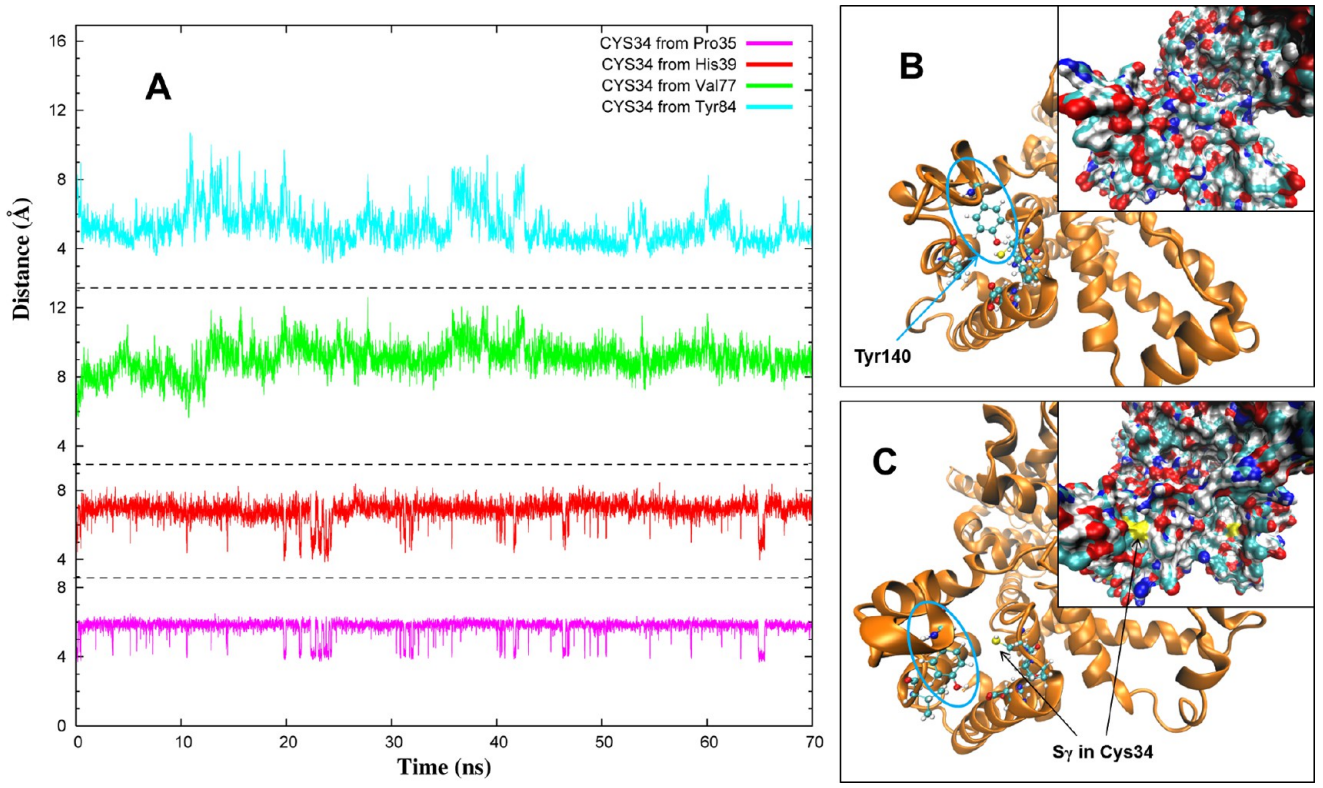

Figure 9. (A) Time evolution of the distances between the Sγ atom in Cys34 and the centers of mass of hindering residues. (B) Snapshots of the crystal structure and (C) snapshot after 60 ns of MD simulation with groups that sterically hinder Sγ in Cys34. Val77 and Tyr84 are flexible groups and can easily sample different conformations. Sγ (yellow atom) is accessible from the surface when Tyr84 (circled) flips over and its phenolic ring moves away from Cys34. Other residues that sterically hinder the surface accessibility to Sγ in Cys34 are Pro35, Asp38, His39, and Val77. Once the sulfhydryl group of Cys34 is on the surface, it can be accessed by sulfhydryl groups of other HSA molecules and form intermolecular linkages.

are a suitable technique for studying changes in structural conformation and dynamics of specific residues in the protein. Simulated structures with SS bonds (i.e., native HSA) were used to determine whether Cys34 becomes exposed to the surface.

Cys34 is located in a coil but surrounded by rigid α-helices. A strong hydrogen bond is formed between Cys34 and Tyr140 with occupancies on the order of 98% (see Table SI.1, Supporting Information), which does not favor a change in backbone conformation. Distances between the Sγ atom in Cys34 and the center of mass of the hindering residues were monitored in the 70-ns simulation and are shown in Figure 9, with selected simulation snapshots in which Cys34 is clearly accessible from the surface, with a probe radius of 1.4 Å. Residues that sterically hinder Cys34 sample different conformations in which the distances between Sγ and the side groups increase, in some cases simultaneously, as in Pro35 and His39. Because of their hydrophobicity and location on the surface of the protein, Val77 and Tyr84 are very mobile and sample a variety of conformations. Tyr84 has significant mobility (*B* factor of 96 Å^2 in the experimental structure), and it can be seen that its phenolic group moves away from the sulfhydryl group, providing access to Cys34 from the surface, as presented in the snapshots of Figure 9. Val77 and Pro35 are located in the extreme of an α-helix next to a coil, but Val77 has a higher experimental *B* factor of 43 Å^2 compared to 30 Å^2 for Pro35. These residues also moved away from Cys34, giving other molecules access to the Sγ atom of Cys34. His39 is located in an α-helix and does not change its conformation significantly. Asp38 also influences the accessibility of Sγ in Cys34, but as in His39, there are no major changes in conformation and dynamics.

Aside from Cys34, most sulfhydryl groups in cysteine are well protected and hardly accessible to the solvent. However, when SS bonds are removed, some sulfhydryl groups are exposed to the surface, such as Cys169, Cys253, Cys265, Cys361, and Cys567. These groups will have better chances of forming intermolecular SS bonds and producing higher-order structures. Aggregation studies in the absence of SS bonds were not performed, but the effect of SS bonds on the conformational stability of the protein and surface accessibility of cysteine residues will likely affect the aggregation propensity of the protein.

3.5. Relations with Functionality and Binding Affinity.

HSA is well-known for its binding affinity to fatty acids and a variety of drugs. Several small heterocyclic and aromatic carboxylic acids bind to the two main sites. These regions form a pocket structure and are essentially hydrophobic, with four SS bonds in each site: Cys200−Cys246, Cys245−Cys253, Cys265−Cys279, and Cys278−Cys289 in binding site I (subdomains IIA) and Cys392−Cys438, Cys437−Cys448, Cys461−Cys477, and Cys476−Cys487 in binding site II (subdomains IIIA). Site I specifically binds to drugs such as aspirin, bilirubin, azapropazone,[77] warfarin (an anticoagulant),[54,59] phenylbutazone and tolbutamide.[51,59] Binding site II has high affinity for tryptophane, diazepam, digitoxin, ibuprofen, thyroxine, and octanoate, among others.[48,51,78] Additionally, HSA binds to fatty acids with a variety of affinities in six different and asymmetrically distributed sites.[61] Although the hydrophobicities and charges of the residues are important

dx.doi.org/10.1021/jp402994r | J. Phys. Chem. B XXXX, XXX, XXX−XXX

for the affinity of drugs and fatty acids, the particular structure of these sites is believed to play an important role in the binding affinity of HSA. Residues in the vicinity of SS bonds have been associated with binding. Reed observed that palmitic acid binds with high affinity to bovine serum albumin and in particular to Lys116, Lys349, and Lys473.[79] The corresponding residues for HSA are Arg117, Lys351, and Lys475; the latter is next to Cys476, and its binding affinity could be affected by the breakage of SS bonds. The following analysis focuses on the main drug binding sites.

B factors in the primary binding sites of HSA (subdomains IIA and IIIA) are quite low, with most fluctuations below 50 Å^2 for both the experimental and simulated structures (see details in Figure 7). The removal of the eight SS bonds in the binding sites did not affect the dynamics and overall structure because of the presence of hydrogen bonds. However, the absence of SS bonds partially affected the pocket structure of these sites. Figure 10 presents a snapshot of binding site I at 60 ns without SS bonds compared to the initial crystal structure. In this site, Cys245 and Cys253 form a SS bond that contributes to keeping the native conformation between α-helices h3 and h4 in subdomain IIA and a flexible coil in Gly248−Asp249. In the absence of SS bonds, this coil is extended, partially changing the secondary structure in the region between Thr243 and Leu260. The structure of site I becomes looser, which could impact its binding capacity. Other SS bonds in the same site did not have analogous effects in the structure, and no major changes in the overall structure were observed when the Cys278−Cys289 bond was broken. In binding site II, similar changes in structure were observed upon the removal of the SS bonds in Cys437 and Cys448, also located in a region of α-helices. Distances sampled by each SS bond in the binding sites are presented in the Supporting Information (Figures SI.1−SI.3).

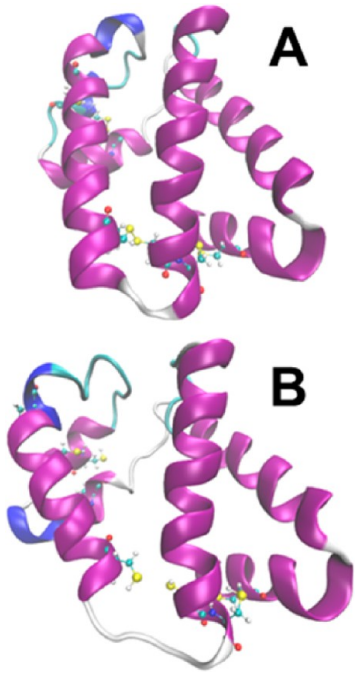

Figure 10. Snapshots of binding site I (subdomain IIA) at (A) 0 and (B) 60 ns without SS bonds. Breaking the SS bond between Cys245 and Cys253 promotes a change in secondary structure, affecting α-helices h3 and h4. This SS bond appears to be important in providing the pocketlike structure of binding site I.

4. CONCLUSIONS

In this work, HSA was selected as a model protein because it plays an important role in the human body and is a "medium-size protein", with 585 residues and 34 cysteine residues participating in SS bonds. SS bonds influence the conformational stability of the native structure, consequently affecting the local dynamics of several regions. These results provide not only detailed information on the importance of SS bonds for HSA, but also the pathway toward understanding other proteins with a rich SS bond structure, such as immunoglobulin G.

Atomistic MD simulations of 70 ns duration of HSA with and without SS bonds revealed specific changes in structure and dynamics that the absence of these interactions might cause. The removal of SS bonds destabilizes the tertiary structure of the protein, but changes occurred only after 35 ns of MD simulation. Some SS bonds (e.g., Cys168−Cys177) are responsible for secondary structure, and in particular, the structure of the binding sites is affected after removal of these SS bonds. On the contrary, some cysteine residues (e.g., Cys200−Cys246) are not responsible for local structure and dynamics, as hydrogen bonds play an important role in maintaining the structure and correlated motions in those regions. These results suggest the presence of redundant interactions such as SS bonds or hydrogen bonds in specific regions of the protein. Nonetheless, SS bonds are essential for the global heart-shaped structure and dynamics of HSA.

Cys34 becomes accessible from the surface as the phenolic group in Tyr84 moves away from the sulfhydryl group. Pro35, Asp38, His39, and Val77 also change their conformations to allow the Sγ atom in Cys34 to participate in intermolecular SS bonds. Significant changes in the backbone conformation of Cys34 rarely occur, because of the prevailing hydrogen bond formed with Tyr140. The trajectories of these simulations contain rich information on the conformational structure and dynamics of HSA and provide the data required for accurate bottom-up coarse-grained models to study phenomena that occur at longer time and length scales than atomistic simulations can achieve (i.e., protein aggregation).

■ ASSOCIATED CONTENT

Supporting Information

Evaluation of the separation distances and fluctuations for all cysteine residues after removal of SS bonds and results from the hydrogen-bond analysis. This material is available free of charge via the Internet at http://pubs.acs.org.

■ AUTHOR INFORMATION

Corresponding Author

*E-mail: colina@matse.psu.edu.

Notes

The authors declare no competing financial interest.

■ ACKNOWLEDGMENTS

The authors are very grateful to MedImmune for providing financial support for this research and to Jai A. Pathak and Ralph H. Colby for establishing this new collaboration between MedImmune LLC and Penn State University. Special thanks are due to Hujun Shen for his valuable input during the start of the simulations and Michael E. Fortunato for his comments on the manuscript. The authors also acknowledge the anonymous reviewers for their comments, especially reviewer 2 for his/her

detailed and helpful comments to strengthen the manuscript. Computational resources for this research were provided by the Materials Simulation Center of the Materials Research Institute, the Research Computing and Cyberinfrastructure unit of Penn State Information Technology Services, and the Penn State Center for Nanoscale Science.

■ ABBREVIATIONS

DCCM, dynamic cross-correlation map; HSA, human serum albumin; MD, molecular dynamics; PDB, Protein Data Bank; PMEMD, particle mesh Ewald molecular dynamics; RMSD, root-mean-square deviation; SS, disulfide

■ REFERENCES

(1) Wang, W.; Roberts, C. J. *Aggregation of Protein Therapeutics*; John Wiley & Sons: Hoboken, NJ, 2010.
(2) Wedemeyer, W. J.; Welker, E.; Narayan, M.; Scheraga, H. A. Disulfide Bonds and Protein Folding. *Biochemistry* **2000**, *39*, 4207−4216.
(3) Watanabe, K.; Nakamura, A.; Fukuda, Y.; Saitô, N. Mechanism of Protein Folding: III. Disulfide Bonding. *Biophys. Chem.* **1991**, *40*, 293−301.
(4) Creighton, T. E. Disulphide Bonds and Protein Stability. *BioEssays* **1988**, *8*, 57−63.
(5) Steudel, R. Properties of Sulfur−Sulfur Bonds. *Angew. Chem., Int. Ed.* **1975**, *14*, 655−664.
(6) Carrotta, R.; Manno, M.; Giordano, F. M.; Longo, A.; Portale, G.; Martorana, V.; Biagio, P. L. S. Protein Stability Modulated by a Conformational Effector: Effects of Trifluoroethanol on Bovine Serum Albumin. *Phys. Chem. Chem. Phys.* **2009**, *11*, 4007−4018.
(7) Wilkinson, B.; Gilbert, H. F. Protein Disulfide Isomerase. *Biochim. Biophys. Acta* **2004**, *1699*, 35−44.
(8) Anfinsen, C. B.; Haber, E. Studies on the Reduction and Re-Formation of Protein Disulfide Bonds. *J. Biol. Chem.* **1961**, *236*, 1361−1363.
(9) Karlin, A.; Bartels, E. Effects of Blocking Sulfhydryl Groups and of Reducing Disulfide Bonds on the Acetylcholine-Activated Permeability System of the Electroplax. *Biochim. Biophys. Acta* **1966**, *126*, 525−535.
(10) Sun, T. T.; Green, H. Keratin Filaments of Cultured Human Epidermal Cells. Formation of Intermolecular Disulfide Bonds during Terminal Differentiation. *J. Biol. Chem.* **1978**, *253*, 2053−2060.
(11) Cooper, A.; Eyles, S. J.; Radford, S. E.; Dobson, C. M. Thermodynamic Consequences of the Removal of a Disulphide Bridge from Hen Lysozyme. *J. Mol. Biol.* **1992**, *225*, 939−943.
(12) Drakopoulou, E.; Vizzavona, J.; Neyton, J.; Aniort, V.; Bouet, F.; Virelizier, H.; Menez, A.; Vita, C. Consequence of the Removal of Evolutionary Conserved Disulfide Bridges on the Structure and Function of Charybdotoxin and Evidence That Particular Cysteine Spacings Govern Specific Disulfide Bond Formation. *Biochemistry* **1998**, *37*, 1292−1301.
(13) Siddiqui, K. S.; Poljak, A.; Guilhaus, M.; Feller, G.; D'Amico, S.; Gerday, C.; Cavicchioli, R. Role of Disulfide Bridges in the Activity and Stability of a Cold-Active α-Amylase. *J. Bacteriol.* **2005**, *187*, 6206−6212.
(14) Vaz, D. C.; Rodrigues, J. R.; Sebald, W.; Dobson, C. M.; Brito, R. M. M. Enthalpic and Entropic Contributions Mediate the Role of Disulfide Bonds on the Conformational Stability of Interleukin-4. *Protein Sci.* **2006**, *15*, 33−44.
(15) Godwin, A.; Choi, J.-W.; Pedone, E.; Balan, S.; Jumnah, R.; Shaunak, S.; Brocchini, S.; Zloh, M. Molecular Dynamics Simulations of Proteins with Chemically Modified Disulfide Bonds. *Theor. Chem. Acc.* **2007**, *117*, 259−265.
(16) Moghaddam, M. E.; Naderi-Manesh, H. Role of Disulfide Bonds in Modulating Internal Motions of Proteins to Tune Their Function: Molecular Dynamics Simulation of Scorpion Toxin Lqh III. *Proteins: Struct., Funct., Bioinf.* **2006**, *63*, 188−196.
(17) Qin, M.; Zhang, J.; Wang, W. Effects of Disulfide Bonds on Folding Behavior and Mechanism of the β-Sheet Protein Tendamistat. *Biophys. J.* **2006**, *90*, 272−286.
(18) Tsai, Y.-L.; Chen, H.-W.; Lin, T.; Wang, W.-Z.; Sun, Y.-C. Molecular Dynamics Simulation of Folding of a Short Helical Toxin Peptide. *J. Theor. Comput. Chem.* **2007**, *06*, 213−221.
(19) Aschi, M.; Bozzi, A.; Di Bartolomeo, R.; Petruzzelli, R. The Role of Disulfide Bonds and N-Terminus in the Structural Properties of Hepcidins: Insights from Molecular Dynamics Simulations. *Biopolymers* **2010**, *93*, 917−926.
(20) Allison, J. R.; Moll, G.-P.; van Gunsteren, W. F. Investigation of Stability and Disulfide Bond Shuffling of Lipid Transfer Proteins by Molecular Dynamics Simulation. *Biochemistry* **2010**, *49*, 6916−6927.
(21) Clarke, J.; Hounslow, A. M.; Fersht, A. R.; Bond, C. J.; Daggett, V. The Effects of Disulfide Bonds on the Denatured State of Barnase. *Protein Sci.* **2000**, *9*, 2394−2404.
(22) Betz, S. F. Disulfide Bonds and the Stability of Globular Proteins. *Protein Sci.* **1993**, *2*, 1551−1558.
(23) Zavodszky, M.; Chen, C. W.; Huang, J. K.; Zolkiewski, M.; Wen, L.; Krishnamoorthi, R. Disulfide Bond Effects on Protein Stability: Designed Variants of Cucurbita Maxima Trypsin Inhibitor-V. *Protein Sci.* **2001**, *10*, 149−160.
(24) Ramm, K.; Gehrig, P.; Pluckthun, A. Removal of the Conserved Disulfide Bridges from the scFv Fragment of an Antibody: Effects on Folding Kinetics and Aggregation. *J. Mol. Biol.* **1999**, *290*, 535−546.
(25) Liu, H.; May, K. Disulfide Bond Structures of IgG Molecules: Structural Variations, Chemical Modifications and Possible Impacts to Stability and Biological Function. *mAbs* **2012**, *4*, 17−23.
(26) Cho, S. S.; Levy, Y.; Onuchic, J. N.; Wolynes, P. G. Overcoming Residual Frustration in Domain-Swapping: The Roles of Disulfide Bonds in Dimerization and Aggregation. *Phys. Biol.* **2005**, *2*, S44.
(27) Furukawa, Y.; Fu, R.; Deng, H.-X.; Siddique, T.; O'Halloran, T. V. Disulfide Cross-Linked Protein Represents a Significant Fraction of ALS-Associated Cu, Zn-Superoxide Dismutase Aggregates in Spinal Cords of Model Mice. *Proc. Natl. Acad. Sci. U.S.A.* **2006**, *103*, 7148−7153.
(28) Niwa, J.-i.; Yamada, S.-i.; Ishigaki, S.; Sone, J.; Takahashi, M.; Katsuno, M.; Tanaka, F.; Doyu, M.; Sobue, G. Disulfide Bond Mediates Aggregation, Toxicity, and Ubiquitylation of Familial Amyotrophic Lateral Sclerosis-Linked Mutant SOD1. *J. Biol. Chem.* **2007**, *282*, 28087−28095.
(29) Van Buren, N.; Rehder, D.; Gadgil, H.; Matsumura, M.; Jacob, J. Elucidation of Two Major Aggregation Pathways in an IgG2 Antibody. *J. Pharm. Sci.* **2009**, *98*, 3013−3030.
(30) Ciaccio, N. A.; Laurence, J. S. Effects of Disulfide Bond Formation and Protein Helicity on the Aggregation of Activating Transcription Factor 5. *Mol. Pharmaceutics* **2009**, *6*, 1205−1215.
(31) Brych, S. R.; Gokarn, Y. R.; Hultgen, H.; Stevenson, R. J.; Rajan, R.; Matsumura, M. Characterization of Antibody Aggregation: Role of Buried, Unpaired Cysteines in Particle Formation. *J. Pharm. Sci.* **2010**, *99*, 764−781.
(32) Shen, H.; Moustafa, I. M.; Cameron, C. E.; Colina, C. M. Exploring the Dynamics of Four RNA-Dependent RNA Polymerases by a Coarse-Grained Model. *J. Phys. Chem. B* **2012**, *116*, 14515−14524.
(33) Chennamsetty, N.; Voynov, V.; Kayser, V.; Helk, B.; Trout, B. L. Design of Therapeutic Proteins with Enhanced Stability. *Proc. Natl. Acad. Sci. U.S.A.* **2009**, *106*, 11937−11942.
(34) Chennamsetty, N.; Voynov, V.; Kayser, V.; Helk, B.; Trout, B. L. Prediction of Aggregation Prone Regions of Therapeutic Proteins. *J. Phys. Chem. B* **2010**, *114*, 6614−6624.
(35) Case, D. A.; Darden, T. A.; Cheatham, T. E., III; Simmerling, C. L.; Wang, J.; Duke, R. E.; Luo, R.; Walker, R. C.; Zhang, W.; Merz, K. M.; Roberts, B.; Hayik, S.; Roitberg, A.; Seabra, G.; Swails, J.; Goetz, A. W.; Kolossváry, I.; Wong, K. F.; Paesani, F.; Vanicek, J.; Wolf, R. M.; Liu, J.; Wu, X.; Brozell, S. R.; Steinbrecher, T.; Gohlke, H.; Cai, Q.; Ye, X.; Wang, J.; Hsieh, M.-J.; Cui, G.; Roe, D. R.; Mathews, D. H.; Seetin, M. G.; Salomon-Ferrer, R.; Sagui, C.; Babin, V.; Luchko, T.; Gusarov,

S.; Kovalenko, A.; Kollman, P. A. *AMBER 12*; University of California, San Francisco, CA, 2012.
(36) Götz, A. W.; Williamson, M. J.; Xu, D.; Poole, D.; Le Grand, S.; Walker, R. C. Routine Microsecond Molecular Dynamics Simulations with Amber on GPUs. 1. Generalized Born. *J. Chem. Theory Comput.* **2012**, *8*, 1542−1555.
(37) Sugio, S.; Kashima, A.; Mochizuki, S.; Noda, M.; Kobayashi, K. Crystal Structure of Human Serum Albumin at 2.5 Å Resolution. *Protein Eng.* **1999**, *12*, 439−446.
(38) Berendsen, H. J. C.; Postma, J. P. M.; van Gunsteren, W. F.; DiNola, A.; Haak, J. R. Molecular Dynamics with Coupling to an External Bath. *J. Chem. Phys.* **1984**, *81*, 3684−3690.
(39) Pastor, R. W.; Brooks, B. R.; Szabo, A. An Analysis of the Accuracy of Langevin and Molecular Dynamics Algorithms. *Mol. Phys.* **1988**, *65*, 1409−1419.
(40) Loncharich, R. J.; Brooks, B. R.; Pastor, R. W. Langevin Dynamics of Peptides: The Frictional Dependence of Isomerization Rates of *N*-Acetylalanyl-*N*′-Methylamide. *Biopolymers* **1992**, *32*, 523−535.
(41) Jesus, A. I.; Daniel, P. C.; Justin, M. W.; Robert, D. S. Langevin Stabilization of Molecular Dynamics. *J. Chem. Phys.* **2001**, *114*, 2090−2098.
(42) Ryckaert, J.-P.; Ciccotti, G.; Berendsen, H. J. C. Numerical Integration of the Cartesian Equations of Motion of a System with Constraints: Molecular Dynamics of *n*-Alkanes. *J. Comput. Phys.* **1977**, *23*, 327−341.
(43) Darden, T.; York, D.; Pedersen, L. Particle Mesh Ewald: An $N \cdot \log(N)$ Method for Ewald Sums in Large Systems. *J. Chem. Phys.* **1993**, *98*, 10089−10092.
(44) Essmann, U.; Perera, L.; Berkowitz, M. L.; Darden, T.; Lee, H.; Pedersen, L. G. A Smooth Particle Mesh Ewald Method. *J. Chem. Phys.* **1995**, *103*, 8577−8593.
(45) Crowley, M.; Darden, T.; Cheatham, T., III; Deerfield, D., II Adventures in Improving the Scaling and Accuracy of a Parallel Molecular Dynamics Program. *J. Supercomput.* **1997**, *11*, 255−278.
(46) Ancell, H. Course of Lectures on the Physiology and Pathology of the Blood and the Other Animal Fluids. *Lancet* **1839−40**, *34*, 916−923.
(47) Rothschild, M. A.; Oratz, M.; Schreiber, S. S. Serum Albumin. *Hepatology* **1988**, *8*, 385−401.
(48) Carter, D. C.; Ho, J. X. Structure of Serum Albumin. *Adv. Protein Chem.* **1994**, *45*, 153−203.
(49) Kratz, F. Albumin as a Drug Carrier: Design of Prodrugs, Drug Conjugates and Nanoparticles. *J. Controlled Release* **2008**, *132*, 171−183.
(50) Rozga, M.; Bal, W. The Cu(II)/Aβ/Human Serum Albumin Model of Control Mechanism for Copper-Related Amyloid Neurotoxicity. *Chem. Res. Toxicol.* **2010**, *23*, 298−308.
(51) Sudlow, G.; Birkett, D. J.; Wade, D. N. Further Characterization of Specific Drug Binding Sites on Human Serum Albumin. *Mol. Pharmacol.* **1976**, *12*, 1052−1061.
(52) Burke, T. G.; Mi, Z. The Structural Basis of Camptothecin Interactions with Human Serum Albumin: Impact on Drug Stability. *J. Med. Chem.* **1994**, *37*, 40−46.
(53) Neault, J. F.; Tajmir-Riahi, H. A. Interaction of Cisplatin with Human Serum Albumin. Drug Binding Mode and Protein Secondary Structure. *Biochim. Biophys. Acta* **1998**, *1384*, 153−159.
(54) Frostell-Karlsson, A.; Remaeus, A.; Roos, H.; Andersson, K.; Borg, P.; Hamalainen, M.; Karlsson, R. Biosensor Analysis of the Interaction between Immobilized Human Serum Albumin and Drug Compounds for Prediction of Human Serum Albumin Binding Levels. *J. Med. Chem.* **2000**, *43*, 1986−1992.
(55) Sulkowska, A. Interaction of Drugs with Bovine and Human Serum Albumin. *J. Mol. Struct.* **2002**, *614*, 227−232.
(56) Ghuman, J.; Zunszain, P. A.; Petitpas, I.; Bhattacharya, A. A.; Otagiri, M.; Curry, S. Structural Basis of the Drug-Binding Specificity of Human Serum Albumin. *J. Mol. Biol.* **2005**, *353*, 38−52.
(57) Liu, H.; Bao, W.; Ding, H.; Jang, J.; Zou, G. Binding Modes of Flavones to Human Serum Albumin: Insights from Experimental and Computational Studies. *J. Phys. Chem. B* **2010**, *114*, 12938−12947.
(58) Zsila, F.; Bikadi, Z.; Malik, D.; Hari, P.; Pechan, I.; Berces, A.; Hazai, E. Evaluation of Drug−Human Serum Albumin Binding Interactions with Support Vector Machine Aided Online Automated Docking. *Bioinformatics* **2011**, *27*, 1806−1813.
(59) Petitpas, I.; Bhattacharya, A. A.; Twine, S.; East, M.; Curry, S. Crystal Structure Analysis of Warfarin Binding to Human Serum Albumin. Anatomy of Drug Site I. *J. Biol. Chem.* **2001**, *276*, 22804−22809.
(60) Carter, D. C.; He, X.-m.; Munson, S. H.; Twigg, P. D.; Gernert, K. M.; Broom, M. B.; Miller, T. Y. Three-Dimensional Structure of Human Serum Albumin. *Science* **1989**, *244*, 1195−1198.
(61) Curry, S.; Mandelkow, H.; Brick, P.; Franks, N. Crystal Structure of Human Serum Albumin Complexed with Fatty Acid Reveals an Asymmetric Distribution of Binding Sites. *Nat. Struct. Biol.* **1998**, *5*, 827−835.
(62) Peters, T. Serum Albumin. *Adv. Protein Chem.* **1985**, *37*, 161−245.
(63) Wardell, M.; Wang, Z.; Ho, J. X.; Robert, J.; Ruker, F.; Ruble, J.; Carter, D. C. The Atomic Structure of Human Methemalbumin at 1.9 Å. *Biochem. Biophys. Res. Commun.* **2002**, *291*, 813−819.
(64) Humphrey, W.; Dalke, A.; Schulten, K. VMD: Visual Molecular Dynamics. *J. Molec. Graphics* **1996**, *14*, 33−38.
(65) Luetscher, J. A. Serum Albumin. II. Identification of More Than One Albumin in Horse and Human Serum by Electrophoretic Mobility in Acid Solution. *J. Am. Chem. Soc.* **1939**, *61*, 2888−2890.
(66) Foster, J. F. *The Plasma Proteins: Isolation, Characterization, and Function*; Academic Press: New York, 1960; Vol. *1*.
(67) Li, J.; Zhu, X.; Yang, C.; Shi, R. Characterization of the Binding of Angiotensin II Receptor Blockers to Human Serum Albumin Using Docking and Molecular Dynamics Simulation. *J. Mol. Model.* **2010**, *16*, 789−798.
(68) Fujiwara, S. I.; Amisaki, T. Molecular Dynamics Study of Conformational Changes in Human Serum Albumin by Binding of Fatty Acids. *Proteins: Struct., Funct., Bioinf.* **2006**, *64*, 730−739.
(69) Sudhamalla, B.; Gokara, M.; Ahalawat, N.; Amooru, D. G.; Subramanyam, R. Molecular Dynamics Simulation and Binding Studies of β-Sitosterol with Human Serum Albumin and Its Biological Relevance. *J. Phys. Chem. B* **2010**, *114*, 9054−9062.
(70) Rueda, M.; Ferrer-Costa, C.; Meyer, T.; Perez, A.; Camps, J.; Hospital, A.; Gelpi, J. L.; Orozco, M. A Consensus View of Protein Dynamics. *Proc. Natl. Acad. Sci. U.S.A.* **2007**, *104*, 796−801.
(71) Deeb, O.; Rosales-Hernández, M. C.; Gómez-Castro, C.; Garduño-Juárez, R.; Correa-Basurto, J. Exploration of Human Serum Albumin Binding Sites by Docking and Molecular Dynamics Flexible Ligand−Protein Interactions. *Biopolymers* **2010**, *93*, 161−170.
(72) Artali, R.; Bombieri, G.; Calabi, L.; Del Pra, A. A Molecular Dynamics Study of Human Serum Albumin Binding Sites. *Farmaco* **2005**, *60*, 485−495.
(73) Bhattacharya, A. A.; Curry, S.; Franks, N. P. Binding of the General Anesthetics Propofol and Halothane to Human Serum Albumin. *J. Biol. Chem.* **2000**, *275*, 38731−38738.
(74) Kabsch, W.; Sander, C. Dictionary of Protein Secondary Structure: Pattern Recognition of Hydrogen-Bonded and Geometrical Features. *Biopolymers* **1983**, *22*, 2577−2637.
(75) Frishman, D.; Argos, P. Knowledge-Based Protein Secondary Structure Assignment. *Proteins: Struct., Funct., Genet.* **1995**, *23*, 566−579.
(76) Ichiye, T.; Karplus, M. Collective Motions in Proteins: A Covariance Analysis of Atomic Fluctuations in Molecular Dynamics and Normal Mode Simulations. *Proteins: Struct., Funct., Bioinf.* **1991**, *11*, 205−217.
(77) Fehske, K. J.; Schlafer, U.; Wollert, U.; Muller, W. E. Characterization of an Important Drug-Binding Area on Human Serum Albumin Including the High-Affinity Binding Sites of Warfarin and Azapropazone. *Mol. Pharmacol.* **1982**, *21*, 387−393.

(78) Sudlow, G.; Birkett, D. J.; Wade, D. N. The Characterization of Two Specific Drug Binding Sites on Human Serum Albumin. *Mol. Pharmacol.* **1975**, *11*, 824−832.
(79) Reed, R. G. Location of Long-Chain Fatty Acid-Binding Sites of Bovine Serum Albumin by Affinity Labeling. *J. Biol. Chem.* **1986**, *261*, 5619−5624.